## Title

The myeloid heat shock transcription factor 1/β-catenin axis regulates NLR family, pyrin domain-containing 3 inflammasome activation in mouse liver ischemia/reperfusion injury.



## Journal

Hepatology, 64(5)

## Authors

Yue, Shi
Zhu, Jianjun
Zhang, Ming
et al.

## Publication Date

2016-11-01

## DOI

10.1002/hep.28739

Peer reviewed

HHS Public Access

Author manuscript

*Hepatology*. Author manuscript; available in PMC 2017 November 01.

Published in final edited form as:

*Hepatology*. 2016 November ; 64(5): 1683–1698. doi:10.1002/hep.28739.

# THE MYELOID HSF1-β-CATENIN AXIS REGULATES NLRP3 INFLAMMASOME ACTIVATION IN MOUSE LIVER ISCHEMIA/ REPERFUSION INJURY

**Shi Yue**[1,4], **Jianjun Zhu**[2,4], **Ming Zhang**[2], **Changyong Li**[1], **Xingliang Zhou**[3], **Min Zhou**[1], **Michael Ke**[1], **Ronald W. Busuttil**[1], **Qi-Long Ying**[3], **Jerzy W. Kupiec-Weglinski**[1], **Qiang Xia**[2], and **Bibo Ke**[1]

[1]The Dumont-UCLA Transplant Center, Division of Liver and Pancreas Transplantation, Department of Surgery, David Geffen School of Medicine at UCLA, Los Angeles, CA, USA

[2]Department of Liver Surgery, Renji Hospital, Shanghai Jiaotong University School of Medicine, Shanghai, China

[3]Eli and Edythe Broad Center for Regenerative Medicine and Stem Cell Research at USC, Department of Stem Cell Biology & Regenerative Medicine, Keck School of Medicine, University of Southern California, Los Angeles, CA, USA

## Abstract

Heat shock transcription factor 1 (HSF1) has been implicated in the differential regulation of cell stress and disease states. β-catenin activation is essential for immune homeostasis. However, little is known about the role of macrophage HSF1-β-catenin signaling in the regulation of NLRP3 inflammasome activation during ischemia and reperfusion injury (IRI) in the liver. This study investigated the functions and molecular mechanisms by which HSF1-β-catenin signaling influenced the NLRP3-mediated innate immune response *in vivo* and *in vitro*. Using a mouse model of IR-induced liver inflammatory injury, we found that mice with a myeloid specific HSF1 knockout ($HSF1^{M\text{-}KO}$) displayed exacerbated liver damage based on their increased serum ALT levels, intrahepatic macrophage/neutrophil trafficking, and pro-inflammatory IL-1β levels compared to the HSF1-proficient ($HSF1^{FL/FL}$) controls. Disruption of myeloid HSF1 markedly increased transcription factor X-box-binding protein (XBP1), NLRP3 and cleaved caspase-1 expression, which was accompanied by reduced β-catenin activity. Knockdown of XBP1 in HSF1-deficient livers using a XBP1 siRNA ameliorated hepatocellular functions and reduced the NLRP3/cleaved caspase-1 and IL-1β protein levels. In parallel *in vitro* studies, HSF1 overexpression increased β-catenin (Ser552) phosphorylation and decreased reactive oxygen species (ROS) production in bone marrow-derived macrophages. However, myeloid HSF1 ablation inhibited β-catenin but promoted XBP1. Furthermore, myeloid β-catenin deletion increased XBP1 mRNA splicing, whereas a CRISPR/Cas9-mediated XBP1 knockout diminished NLRP3/ caspase-1. Conclusions: The myeloid HSF1-β-catenin axis controlled NLRP3 activation by

Contact: Bibo Ke, The Dumont-UCLA Transplant Center, Department of Surgery, David Geffen School of Medicine at UCLA, 77-120 CHS, 10833 Le Conte Ave, Los Angeles, CA 90095. Tel: (310) 794-7557; Fax: (310) 267-2367; bke@mednet.ucla.edu; or Qiang Xia, Department of Liver Surgery, Renji Hospital, Shanghai Jiaotong University School of Medicine, 160 Pujian Road, Shanghai 200127, China. Tel: 86-21-68383775, Fax: 86-21-58737232, xiaqiang@shsmu.edu.cn.

[4]These authors contributed equally to this work.

modulating the XBP1 signaling pathway. HSF1 activation promoted β-catenin, which in turn inhibited XBP1, leading to NLRP3 inactivation and reduced IR-induced liver injury. Our findings demonstrated that HSF1-β-catenin signaling is a novel regulator of innate immunity in liver inflammatory injury and implied the therapeutic potential for the management of sterile liver inflammation in transplant recipients.

**Keywords**

Innate Immunity; ROS; TLR4; XBP1; Liver Injury

Hepatic dysfunction or failure caused by ischemia-reperfusion injury (IRI) is a major problem following liver transplantation (1). Oxidative stress has been recognized as an important factor in the pathogenesis of hepatic IRI (2). Hepatic IR activates liver macrophages (Kupffer cells) to generate reactive oxygen species (ROS), leading to sterile inflammation in the liver. Indeed, ROS functions as an alarm signal that triggers efficient defense responses by modulating specific signal transduction pathways. One signaling pathway that leads to ROS production triggers NLRP3 inflammasome activity (3, 4).

NLRP3 is a member of the NLR family of cytosolic pattern recognition receptors. NLRP3 mediates caspase-1 activation with the adaptor protein ASC to induce the maturation and secretion of IL-1β in response to various pathogen-associated molecular patterns (PAMPs) and danger-associated molecular patterns (DAMPs) released from stressed or injured cells (5). The active NLRP3 inflammasome drives the innate immune response towards invading pathogens and cellular damage and regulates the adaptive immune response (6, 7). A number of human heritable and acquired diseases with dysregulated inflammasome activity have strongly highlighted the importance of the NLRP3 inflammasome in the regulation of immune responses (8). As a danger signal sensor, NLRP3 is essential for the initiation of profound sterile inflammatory injury (9, 10).

Recently, heat shock transcription factor 1 (HSF1), which is a transcription factor for heat shock proteins (HSPs), was shown to facilitate cell survival and proliferation against severe stress insults (11). Indeed, HSF1 is induced by various stressors, including oxidative stress. In unstressed cells, HSF1 is bound in the cytoplasm and forms multimeric protein complexes containing either HSP40/70 or HSP90. When stress causes protein unfolding, HSF1 is released from the complex and translocated to the nucleus, where it binds a heat shock response element to induce transcriptional activity (12). HSF1 overexpression protected cardiomyocytes and improved cell survival against stress-mediated cell apoptosis (13). Increased HSF1 expression promoted anti-inflammatory IL-10 activity and diminished proinflammatory cytokine expression in macrophages (14). Additionally, HSF1 conferred protection against inflammatory injury and bacterial infection (15, 16). Induction of HSF1 prevented LPS-induced liver damage via inhibiting HSP90-mediated inflammatory response (17). We previously found that signal transducer and activator of transcription-3 (STAT3)-induced β-catenin inhibited TLR4-driven inflammatory response in liver IRI (18). The induction of the TLR4-mediated innate immune response was dependent on the activation of the transcription factor X-box binding protein 1 (XBP1) in macrophages (19). Indeed, XBP1

is a key component of the endoplasmic reticulum (ER) stress response that is required for optimal and sustained production of proinflammatory cytokines during the inflammatory response (19). XBP1 deficiency in mice increased their susceptibility to bacterial infections and impaired host defenses (19). Furthermore, engagement of TLR4 and tumor necrosis factor receptor-associated factor 6 (TRAF6) is crucial for mitochondrial/cellular ROS generation (20), which is required for NLRP3 activation (3). Disruption of NLRP3 or its adaptor protein ASC depressed caspase-1 activity and IL-1β production, resulting in reduced IR-triggered liver inflammation (10, 21). Although the roles of HSF1 in the protection of cells and organisms against severe stress insults have been established (16, 22), whether and how HSF1-β-catenin signaling regulates NLRP3 inflammasome activation in liver IRI are unknown.

Here, we identified a novel functional role and regulatory mechanism of HSF1-β-catenin signaling on the NLRP3-mediated innate immune response in liver sterile inflammatory injury. We demonstrated that activation of myeloid HSF1 modulated the liver inflammatory response by promoting β-catenin signaling and depressing XBP1, which in turn inhibited NLRP3 activation and reduced IR-triggered liver inflammatory injury.

## Materials and Methods

### Animals

Floxed HSF1 ($HSF1^{FL/FL}$) and β-catenin ($\beta\text{-catenin}^{FL/FL}$) mice and mice expressing the Cre recombinase under the control of the Lysozyme M (LysM) promoter (LysM-Cre) were used to generate myeloid-specific HSF1 ($HSF1^{M\text{-}KO}$) and β-catenin knockout ($\beta\text{-catenin}^{M\text{-}KO}$) mice. This study was performed in strict accordance with the recommendations in the *Guide for the Care and Use of Laboratory Animals* published by the NIH. The study protocols were approved by the Institutional Animal Care and Use Committee (IACUC) of the University of California at Los Angeles and Shanghai Jiaotong University in China. See Supplementary Materials.

### Mouse liver IRI model and treatment

We used an established mouse model of warm hepatic ischemia followed by reperfusion, as previously described (23). Some animals were injected via their tail veins 4 h prior to ischemia with an Alexa Fluor488-labeled non-specific (control) siRNA, XBP1 siRNAs or NLRP3 siRNA (2 mg/kg) mixed with mannose-conjugated polymers at a ratio determined according to the manufacturer's instructions as previously described (24). See Supplementary Materials.

### Hepatocellular function assay

The serum alanine aminotransferase (sALT) levels, which are an indicator of hepatocellular injury, were measured by IDEXX Laboratories (Westbrook, ME, USA).

### Histology, immunohistochemistry, and immunofluorescence staining

Liver sections were stained with hematoxylin and eosin (H&E). The IRI severity was graded using Suzuki's criteria (25). Liver macrophages and neutrophils were detected using primary

rat anti-mouse $CD11b^+$ and Ly6G mAbs (BD Biosciences, San Jose, CA). Immunofluorescence staining was used to identify *in vivo* mannose-mediated delivery of the siRNA into macrophages. See Supplementary Materials.

### Quantitative RT-PCR analysis

Quantitative real-time PCR was performed as previously described (26). The primer sequences used for the amplification are shown in Supplementary Table 1. See Supplementary Materials.

### Western blotting analysis

Protein was extracted from the liver tissue or cell cultures as previously described (26). The polyclonal rabbit anti-mouse phos-IRE1α, monoclonal rabbit anti-mouse HSF1, phos-β-catenin, β-catenin, phos-Stat3, TLR4, TRAF6, XBP1s, NLRP3, cleaved caspase-1, and β-actin Abs were used. See Supplementary Materials.

### Lentiviral vector production

The pSIN-β-catenin vector expresses β-catenin and contains an EF2 promoter and a puromycin gene (27). The pLJM1-GFP vector contains CMV-driven GFP. pSPAX2 and pCMV-VSV-G are lentiviral packaging plasmids. 293T Cells were co-transfected with pSin-β-catenin (or pLJM1-GFP), pSPAX2, and pCMV-VSV-G using the Lipofectamine LTX Plus reagent to package lentiviruses according to the manufacturer's instructions. See Supplementary Materials.

The lentiviral CRISPR XBP1 knockout vector was constructed by first cloning the XBP1 single guide RNA (sgRNA) sequences into the site of *BsmB*I of the LentiCRISPRv2 vector as previously described (28). Lentiviral vector production was performed as described above. LentiCRISPRv2-XBP1 KO (LV-CRISPR-XBP1 KO), pSPAX2, and pCMV-VSV-G were used to package the viruses. The pLJM1-GFP virus was used as a control. See Supplementary Materials.

### Isolation of hepatocytes and liver Kupffer cells

Primary hepatocytes and liver Kupffer cells were isolated from the $HSF1^{FL/FL}$ and $HSF1^{M\text{-}KO}$ mice as previously described (26, 29). The purity of the Kupffer cells in ischemic liver was 80% based on immunofluorescence staining for $CD11b^+$. See Supplementary Materials.

### BMM isolation and in vitro transfection

Murine bone marrow-derived macrophages (BMMs) were generated as previously described (30). Cells ($1\times10^6$/well) cultured for 7 days were transfected with pBabe-HSF1 or the control vector. In some experiments, the cells were transduced with a lentivirus expressing β-catenin, the CRISPR/Cas9 XBP1 knockout, or the pLJM1-GFP vector. See Supplementary Materials.

### ELISA assay

Murine BMMs culture supernatants were harvested for cytokine analysis. ELISA kits were used to measure the IL-1β, TNF-α, and CXCL-10 levels.

### Reactive oxygen species (ROS) assay

ROS production in the BMMs was measured using the Carboxy-H2DFFDA kit. ROS production by the BMMs was analyzed and quantified by fluorescence microscopy according to the manufacturer's instructions. See Supplementary Materials.

### Caspase-1 enzyme activity assay

Caspase-1 enzymatic activity in BMMs from the β-catenin$^{FL/FL}$, β-catenin$^{M\text{-}KO}$, and HSF1$^{M\text{-}KO}$ mice was determined using a colorimetric assay kit as previously described (21). See Supplementary Materials.

### Statistical analysis

Data were expressed as the mean±SD and analyzed using the Permutation *t*-test and Pearson correlation. Per comparison two-sided *p* values less than 0.05 were considered statistically significant. Multiple group comparisons were performed using one-way ANOVA followed by Bonferroni's post hoc test. We applied Welch's ANOVA to perform multiple group comparisons when the groups showed unequal variances. All analyses were performed using the SAS/STAT software, version 9.4.

## Results

### Myeloid-specific HSF1 deficiency increases hepatocellular damage in liver IRI

The mouse livers from the myeloid-specific HSF1-deficient (HSF1$^{M\text{-}KO}$) and HSF1-proficient (HSF1$^{FL/FL}$) mice were subjected to 90 min of warm ischemia followed by 6 h of reperfusion. We isolated both hepatocytes and Kupffer cells from these ischemic livers and found that, HSF1$^{M\text{-}KO}$ did not change hepatocyte HSF1 expression. However, the HSF1 expression was undetectable in Kupffer cells from the HSF1$^{M\text{-}KO}$ but not in the HSF1$^{FL/FL}$ mice (Figure 1A). Hepatocellular functions were evaluated by measuring the serum ALT (sALT) levels (IU/L). The sALT levels were increased in the HSF1$^{M\text{-}KO}$ mice compared with the HSF1$^{FL/FL}$ controls (Figure 1B, 8825±714.2 vs. 4765±629.3, $p<0.01$). These data correlated with Suzuki's histological grading of liver IRI. The HSF1$^{FL/FL}$ mouse livers showed mild to moderate edema, sinusoidal congestion, and mild necrosis (Figure 1C, score=2.13±0.08). In contrast, the HSF1$^{M\text{-}KO}$ mouse livers displayed severe edema, sinusoidal congestion, and extensive hepatocellular necrosis (Figure 1C, score=3.65±0.15, $p<0.01$). Consistent with the histopathological and hepatocellular function data, the MPO levels, which reflect liver neutrophil activity (U/g), were significantly elevated in the HSF1$^{M\text{-}KO}$ group but not in the HSF1$^{FL/FL}$ group (Figure 1D, 3.55±0.15 vs. 2.05±0.25, $p<0.01$).

### Myeloid-specific HSF1 deficiency increases macrophage/neutrophil trafficking and proinflammatory mediators in IR-stressed liver

We analyzed macrophage and neutrophil accumulation in IR-stressed livers by immunohistochemistry staining. The $HSF1^{M\text{-}KO}$ ischemic livers exhibited increased $CD11b^{+}$ macrophages infiltration (39.5±1.5) compared to the $HSF1^{FL/FL}$ controls (Figure 2A, 18.3±0.8, $p<0.01$). These results were supported by the real-time PCR analysis in which $HSF1^{M\text{-}KO}$ increased the IL-1β, TNF-α, and CXCL-10 mRNA levels compared to the $HSF1^{FL/FL}$ controls (Figure 2B). Further immunostaining analysis revealed increased neutrophil trafficking in the $HSF1^{M\text{-}KO}$ livers compared to the $HSF1^{FL/FL}$ controls (Figure 2C, 95.6±3.38 vs. 43.6±1.1, $p<0.01$), which was companied by augmented CXCL-1 mRNA levels (Figure 2D).

### Myeloid-specific HSF1 deficiency depresses β-catenin signaling and enhances XBP1/NLRP3 activation in IR-stressed liver

Next, we analyzed whether HSF1 regulated the innate immune response in IR-triggered liver injury. Following 6 h of reperfusion after 90 min of ischemia, $HSF1^{M\text{-}KO}$ augmented spliced XBP1 (XBP1s), NLRP3 and IL-1β mRNA expression in the ischemic livers, as compared with $HSF1^{FL/FL}$ controls (Figure 3A). The Western blotting analysis revealed elevated XBP1s, NLRP3, and cleaved caspase-1 protein levels (Figure 3B) in the $HSF1^{M\text{-}KO}$ livers, which resulted in increased IL-1β, TNF-α, and CXCL-10 production (Figure 3C). Moreover, decreased STAT3 and β-catenin phosphorylation at Ser552 was found in the $HSF1^{M\text{-}KO}$ but not the $HSF1^{FL/FL}$ livers after hepatic IR (Figure 3D). To investigate whether HSF1 specifically influenced β-catenin activation in liver Kupffer cells, we isolated both hepatocytes and Kupffer cells from ischemic livers from the $HSF1^{FL/FL}$ and $HSF1^{M\text{-}KO}$ mice. $HSF1^{M\text{-}KO}$ did not change hepatocyte β-catenin activation. However, reduced Kupffer cell β-catenin phosphorylation was observed in the $HSF1^{M\text{-}KO}$ but not in the $HSF1^{FL/FL}$ mice (Figure 3E).

### NLRP3 activation in myeloid HSF1-deficient liver contributes to IR-triggered liver inflammation

To evaluate whether NLRP3 activation in the $HSF1^{M\text{-}KO}$ livers contributed to IR-induced liver inflammation, we disrupted NLRP3 in the $HSF1^{M\text{-}KO}$ livers using a NLRP3 siRNA with an *in vivo* mannose-mediated delivery system that enhances delivery to cells expressing a mannose-specific membrane receptor to macrophages as previously described (24, 31). Disruption of NLRP3 with the siRNA treatment reduced IR-induced liver damage as evidenced by the decreased Suzuki's histological score (Figure 4A, score=0.95±0.21 vs. 3.75±0.35, $p<0.01$) and sALT levels (Figure 4B, 3931±799 vs. 9014±814, $p<0.01$) compared to the non-specific (NS) siRNA-treated controls. Moreover, NLRP3 siRNA administration in the $HSF1^{M\text{-}KO}$ ischemic livers decreased $CD11b^{+}$ macrophages (Figure 4C, 58.7±11.8 vs. 337.5±23.9, $p<0.01$) and neutrophil (Figure 4D, 32.75±6.26 vs. 117±12.1, $p<0.01$) accumulation compared to the NS siRNA-treated controls. These results were consistent with the ELISA analysis, in which the NLRP3 blockade in $HSF1^{M\text{-}KO}$ reduced serum IL-1β levels (Figure 4E, 88.25±24.7 vs. 380±133.6 $p<0.05$) and liver TNF-α and CXCL-10 mRNA levels compared with the NS siRNA-treated controls (Figure 4F).

### XBP1 is required for NLRP3 activation in myeloid HSF1-deficient liver in response to IR

Because myeloid-specific HSF1 deletion induced XBP1 activation, we examined whether XBP1 affected NLRP3 function in IR-triggered liver inflammation. We disrupted XBP1 in $HSF1^{M\text{-}KO}$ livers using a mannose-mediated XBP1 siRNA *in vivo*. The mannose-mediated AlexaFluor488-labeled siRNA (green) delivery efficiently transduced into macrophages (red) in IR-stressed livers (Figure 5A). Livers in the $HSF1^{M\text{-}KO}$ mice with NS siRNA treatment revealed significant edema, severe sinusoidal congestion/cytoplasmic vacuolization, and extensive (30–50%) necrosis (Figure 4B, score=3.9±0.1). In contrast, the livers in the mice treated with mannose-mediated XBP1 siRNA showed mild to moderate edema without necrosis (Figure 5B, score=2.0±0.1, $p<0.01$). Consistent with these data, the sALT levels were significantly decreased in the XBP1 siRNA-knock down mice compared to the NS siRNA-treated controls (Figure 5C, 3992±190 vs. 10080±722, $p<0.001$). Moreover, XBP1 siRNA treatment in the $HSF1^{M\text{-}KO}$ livers reduced serum IL-1β release (Figure 5D, 175.75±19.3 vs. 360±40.2, $p<0.05$) and NLRP3 and cleaved caspase-1 protein expression (Figure 5E), which were accompanied by decreased IL-1β, TNF-α, and CXCL-10 production compared to the NS siRNA-treated group (Figure 5F).

### Disruption of myeloid HSF1 inhibits β-catenin activity but enhances NLRP3 inflammasome activation in macrophages

Having demonstrated that myeloid HSF1 activates β-catenin signaling to regulate IR-triggered liver inflammation, next we tested the regulatory role of HSF1 during inflammatory response in macrophages. BMMs from WT mice were transfected with the HSF1-expressing vector pBabe-HSF1 or the control vector followed by LPS stimulation. Transfection of pBabe-HSF1 increased the HSF1 mRNA (Supplementary figure 1A) and protein expression levels compared to the controls (Figure 6A). Moreover, overexpression of HSF1 by pBabe-HSF1 transfection increased STAT3 and β-catenin phosphorylation at Ser552 (Figure 6A), which is a site associated with enhanced β-catenin transcriptional activity (32), and decreased IL-1β, TNF-α, and CXCL-10 expression (Figure 6B). Interestingly, pBabe-HSF1-mediated transfection markedly decreased the ROS production in LPS-stimulated macrophages compared to the controls (Figure 6C, 18±1.73 vs. 46.67±2.96, $p<0.01$).

To determine the importance of HSF1 for NLRP3 functions in macrophages, BMMs were isolated from $HSF1^{FL/FL}$ and $HSF1^{M\text{-}KO}$ mice and then cultured with LPS. HSF1 deficiency increased the NLRP3 mRNA expression levels in LPS-stimulated BMMs (Supplementary figure 1B). NLRP3 and cleaved caspase-1 protein expression was consistently increased in the $HSF1^{M\text{-}KO}$ BMMs but not the $HSF1^{FL/FL}$ cells after LPS stimulation (Figure 6D). Moreover, the $HSF1^{M\text{-}KO}$ cells exhibited significantly decreased β-catenin phosphorylation at Ser552 (Figure 6D) accompanied by increased IL-1β, TNF-α, and CXCL-10 production (Figure 6E). Strikingly, the $HSF1^{M\text{-}KO}$ cells displayed significantly increased ROS production compared to the $HSF1^{FL/FL}$ controls (Figure 6F, 78.33±3.28 vs. 46.33±1.85, $p<0.01$) in response to LPS stimulation.

### Myeloid β-catenin signaling is essential for HSF1-mediated immune regulation of NLRP3 functions in macrophages

To elucidate the mechanisms of β-catenin in the HSF1-mediated immune regulation of NLRP3 function, we cultured BMMs from β-catenin$^{FL/FL}$ and β-catenin$^{M-KO}$ mice and then transfected them with the HSF1 expression vector pBabe-HSF1 or the control vector, followed by LPS stimulation. Clearly, pBabe-HSF1 transfection in the β-catenin$^{FL/FL}$ cells markedly increased HSF1 and β-catenin expression but inhibited TLR4 expression (Figure 7A) compared to the control vector-transfected cells. However, the β-catenin$^{M-KO}$ cells exhibited augmented TLR4 expression even though these cells were transfected with pBabe-HSF1 (Figure 7A). Moreover, β-catenin$^{M-KO}$ enhanced NLRP3 activation in BMMs based on the increased NLRP3 mRNA levels (Supplementary Figure 1C) and NLRP3 and cleaved caspase-1 protein expression levels (Figure 7A) and activity (Supplementary Figure 1D). Because transcription factor XBP1 activation is induced by TLR4 signaling and β-catenin is crucial for the regulation of the TLR4-driven inflammatory response in macrophages (18, 19), we investigated spliced XBP1 expression in the β-catenin$^{M-KO}$ cells. Interestingly, β-catenin$^{M-KO}$ increased TRAF6 and IRE1α phosphorylation (Figure 7B), resulting in increased splicing XBP1 mRNA (Supplementary Figure 1E) and protein expression in response to LPS stimulation compared to the β-catenin$^{FL/FL}$ cells (Figure 7B). Furthermore, increased IL-1β production was found in the β-catenin$^{M-KO}$ cells but not in the β-catenin$^{FL/FL}$ cells (Figure 7C, 1101±60.1 vs. 515.7±60.82 $p<0.01$).

### HSF1-β-catenin axis inhibits XBP1-dependent NLRP3 activation in macrophages

To dissect the regulatory mechanisms underlying the effect of the HSF1-β-catenin axis on NLRP3 functions in macrophages, BMMs from the HSF1$^{M-KO}$ mice were transfected with a lentivirus expressing β-catenin. In contrast to the lentiviral-mediated GFP (LV-pLJM1-GFP) control, transfection of HSF1$^{M-KO}$ cells with the lentivirus expressing β-catenin (pSIN-β-catenin) increased β-catenin expression but inhibited IRE1α, XBP1, NLRP3, and cleaved caspase-1 expression (Figure 7D) in response to LPS stimulation. To determine the role of macrophage XBP1 in NLRP3 activation, we disrupted XBP1 by using a CRISPR/Cas9 XBP1 knockout vector (LV-CRISPR-XBP1 KO) in BMMs from HSF1$^{M-KO}$ mice. Strikingly, knockdown of XBP1 in LV-CRISPR-XBP1 KO-treated cells led to decreased NLRP3 and cleaved caspase-1 expression (Figure 7E), which was confirmed by examining the caspase-1 activity (Supplementary Figure 1F) in response to LPS stimulation compared to the LV-pLJM1-GFP-treated control. Moreover, IL-1β production was decreased in the XBP1 knockdown group but not in the control group (Figure 7F, 1063±96.4 vs. 2638±337, $p<0.01$). Similarly, XBP1 knockdown reduced TNF-α and CXCL-10 expression in the HSF1$^{M-KO}$ BMMs after LPS-stimulation (Supplementary Figure 1G).

## Discussion

To the best of our knowledge, this is the first study to document the key role of the myeloid HSF1-β-catenin axis in the regulation of the NLRP3 inflammasome-mediated innate immune responses in liver sterile inflammatory injury. In this study, we demonstrate the following: i) myeloid HSF1 is essential for the control of liver inflammation through the activation of β-catenin signaling; ii) β-catenin activation inhibits NLRP3/caspase-1

activation and reduces the IL-1β level; and iii) the myeloid HSF1-β-catenin axis regulates NLRP3 functions in an XBP1 dependent manner. Our results highlight the importance of myeloid HSF1 in orchestrating β-catenin signaling, XBP1/NLRP3 activation, and the local sterile inflammation cascade in the IR-stressed liver.

The NLRP3 inflammasome is activated by a wide range of danger signals (5). Generation of ROS by oxidative stress is a crucial element for NLRP3 activation (33). Stress-induced ROS mediates the host-defense response by modulating several signaling pathways to induce NLRP3 activation (3). Previous studies have shown that HSF1 inhibits ROS-mediated cell death by regulating c-Jun N-terminal kinase (JNK) activity (13). We found that HSF1 overexpression increased STAT3 and β-catenin phosphorylation and decreased ROS production in macrophages. Consistent with our previous report that β-catenin regulated the TLR4-mediated inflammatory response by controlling dendritic cell (DC) maturation and functions to program innate and adaptive immunity (18), our present results suggest that β-catenin plays a pivotal role in HSF1-mediated immune regulation.

With the dramatic expression of β-catenin and its potent ability to regulate ROS production in macrophages, HSF1 could act as a native regulator for ROS-induced NLRP3 activation during the inflammatory response. Using BMMs from $HSF1^{M\text{-}KO}$ mice, we found that HSF1 deletion activated NLRP3 and caspase-1, which is a key mediator in the processing of the proinflammatory cytokine IL-1β from an inactive precursor to an active, secreted molecule to trigger the innate immune response (34). Notably, NLRP3 and caspase-1 activation was accompanied by decreased β-catenin phosphorylation in the HSF1-deficient cells after LPS stimulation, suggesting the importance of β-catenin in mediating HSF1-mediated immune regulation of the NLRP3 functions. Further evidence for a role for β-catenin in the control of NLRP3 functions was obtained from myeloid cell-specific β-catenin knockout ($\beta\text{-catenin}^{M\text{-}KO}$) mice. We found that deletion of β-catenin in cells from the $\beta\text{-catenin}^{M\text{-}KO}$ mice reversed the HSF1-mediated inhibition of TLR4, NLRP3, and caspase-1 activation compared to BMMs from the $\beta\text{-catenin}^{FL/FL}$ mice. $\beta\text{-catenin}^{M\text{-}KO}$ increased IR-induced liver damage (Supplementary Figure 3). Indeed, β-catenin signaling has been shown to possess multiple regulatory functions during the inflammatory response. Increasing β-catenin activation may inhibit NF-κB activation or promote PI3K/Akt, leading to inhibition of the innate TLR4-mediated inflammatory response in a negative feedback regulatory mechanism (18). Moreover, TLR4 signaling is relayed by the adapter molecule myeloid differentiation factor 88 (MyD88) and toll/interleukin 1 receptor domain-containing adapter inducing IFN-β (TRIF)-mediated pathways (35). TRIF has been linked to NLRP3 activation by promoting caspase-11 activity during Gram-negative bacterial infection (36). TLR4 stimulation may increase ER stress sensor kinase IRE1α activation (37), indicating that the unfolded protein response may be required for the innate immune response. Interestingly, our data revealed that increasing macrophage β-catenin expression inhibited IRE1α phosphorylation. However, deletion of β-catenin in cells from the $\beta\text{-catenin}^{M\text{-}KO}$ mice increased the activation of IRE1α and its downstream transcription factor XBP1, resulting in augmented NLRP3/caspase-1 activity. Because inflammasome NLRP3/caspase-1 is responsible for the activation of innate immunity, our findings suggest that β-catenin may interact with XBP1 to regulate the innate inflammatory process in macrophages.

The crosstalk between the cellular stress response and innate immune signaling is less clear. Previous studies have demonstrated that the cellular stress caused by oxygen deficiency (hypoxia) induce the inflammatory response associated with ischemic and inflammatory diseases via a hypoxia-inducible transcription factor (HIF) signaling pathway (38). Induction of HIF-1α contributes to cytokine activation and the development of LPS-induced sepsis in a TLR4-dependent manner (39). Moreover, ATP released from intracellular storage under ischemic or hypoxic conditions plays a role as the predominant signaling molecule in triggering inflammatory response through the activation of purinergic P2 receptors (40). Indeed, the purinergic receptor P2X7R has been shown to mediate ATP-driven NLRP3 activation (41), suggesting the convergence of multiple signaling pathways on NLRP3 activation. Cell stress can trigger an innate immune response, such as the ER-stress sensor kinase IRE1α induces XBP1 activation by TLR-mediated signaling pathways (19). β-catenin activation inhibited TLR4 signaling, which implies a functional link between β-catenin and XBP1 in the stress-mediated immune response. In our current study, increased IRE1α phosphorylation and mature XBP1 production were observed in BMMs from β-catenin$^{M\text{-}KO}$ mice in response to TLR4 agonist (LPS) stimulation. However, β-catenin overexpression by lentivirus-mediated transduction suppressed IRE1α-mediated XBP1 activation. IRE1α is a Ser/Thr protein kinase and endoribonuclease that controls the processing of the splicing mRNA encoding XBP1, which forms the potent transcription factor XBPs (42, 43). Using lentivirus CRISPR/Cas9-mediated genome editing, we found that knockout of XBP1 in macrophages inhibited NLRP3/caspase-1 activation and reduced proinflammatory IL-1β. This finding suggests that macrophage XBP1 expression is essential for the NLRP3-mediated innate immune response.

The mechanisms underlying myeloid HSF1-mediated immune regulation appear to involve multiple signaling pathways. Several key factors may contribute to HSF1-mediated immune regulation in IR-triggered liver inflammation. First, upon liver exposure to IR stress, macrophages are critical for the initial uptake of pathogens, such as PAMPs and DAMPs, to trigger inflammation by activating innate TLR4, which activates the stress sensor IRE1α and the spliced form of XBP1 (XBP1s), resulting in increased expression of proinflammatory cytokines. Second, the myeloid specific HSF1-deficient livers exhibited reduced β-catenin activity, leading to augmented IRE1α-mediated XBP1 activation that in turn enhanced NLRP3-mediated innate immunity. Third, neutrophils are also activated during liver IRI by IL-1/TNF-α and contribute to local inflammation. Our results showed that myeloid specific HSF1-deficient livers exhibited increased neutrophil accumulation based on the MPO assay, Ly6G+ staining, CXCL-1 expression. Furthermore, HSF1$^{M\text{-}KO}$ resulted in severe liver damage compared to the HSF1$^{FL/FL}$ controls. Hence, myeloid HSF1 ablation leads to neutrophil activation, which further enhances the hepatic innate immune cascade.

The question arises as to what other mechanisms may confer β-catenin with the ability to selectively affect TLR4-induced XBP1 activation in HSF1-mediated immune regulation. We showed that activation of β-catenin signaling inhibited XBP1 activity in macrophages. Moreover, LPS-induced splicing of XBP1 was dependent on the adaptors MyD88 or TRIF. Both of these adaptors can engage the signaling molecule TRAF6 (44), suggesting that TRAF6 is required for XBP1 activation in response to TLR stimulation. Our results showed that β-catenin deficiency in β-catenin$^{M\text{-}KO}$ macrophages augmented TRAF6 expression and

IRE1α-induced XBP1 activity compared to the β-catenin$^{FL/FL}$ controls. These data were consistent with other reports that TRAF6 activated the NADPH oxidase NOX2, which induced ROS production and shifted the redox balance to trigger IRE1α activation (37, 45). Thus, β-catenin controls IRE1α-induced XBP1 activation through TRAF6 regulation. Consistent with this finding, knockdown of XBP1 with a CRISPR/Cas9 knockout system resulted in reduced NLRP3 and caspase-1 activity, suggesting that IRE1α-induced XBP1 could regulate the innate immune response via a novel mechanism independently of protein misfolding in macrophages. Indeed, increasing evidence demonstrates that IRE1α activates the innate NLRP3 signaling pathways through promoting thioredoxin-interacting protein (TXNIP) in response to ER stress (46). Engagement of XBP1 by a signaling peptide targeting the ER receptor triggers the NLRP3-mediated immune response (47). Our *in vivo* results revealed an unexpected role of XBP1 in controlling the dynamic crosstalk with NLRP3 in HSF1-β-catenin axis-mediated immune regulation.

Based on the emerging function of HSF1 in protection against oxidative stress-induced injury, it is becoming clear that HSF1-β-catenin signaling is a key player in the regulation of immunity during liver IRI. A recent study with small molecule human HSF1 activators, which increased protein translation and HSF1 activation in mammalian cells, demonstrated their therapeutic benefits against inflammatory injury in neurodegenerative disease (48). Thus, the development of HSF1 activators could be a potential intervention for the treatment of IR-induced liver inflammation. Next, patient samples from liver transplantation could be used to provide proof of principle studies for this pathway in transplant patients. By analyzing the levels of HSF1 in these samples, we can use a small molecule human HSF1 activator to test the regulatory role of the HSF1-β-catenin axis in liver transplant patients.

Figure 8 depicts the putative molecular mechanisms by which the myeloid HSF1-β-catenin axis may regulate innate immunity in IR-triggered liver sterile inflammation. Previous studies have suggested that TLR signaling induces IRE1α-mediated XBP1 activation (19). Activation of NLRP3 mediates caspase-1 activation and IL-1β secretion (5). This study reveals the novel signaling pathway by which HSF1-β-catenin axis regulates NLRP3 activation through control of XBP1 activation in liver inflammatory injury. HSF1 can be induced in IR-stressed livers. HSF1 induction increases β-catenin translocation and activity, which inhibits XBP1 activation in response to TLR/TRAF6 stimulation in macrophages. Moreover, inhibition of XBP1 activity diminishes NLRP3 functions, leading to reduced caspase-1 activation, and the maturation and secretion of IL-1β in liver IRI.

In conclusion, we demonstrate that myeloid HSF1 regulates innate immune responses in liver sterile inflammatory injury. HSF1 controls NLRP3 functions by promoting β-catenin signaling and inhibiting XBP1 activation in the IR-stressed liver. By identifying the molecular pathways by which HSF1 regulates NLRP3-mediated innate immunity, our findings provide the rationale for novel therapeutic approaches to ameliorate IR-triggered liver inflammation and injury.

## Supplementary Material

Refer to Web version on PubMed Central for supplementary material.

## Acknowledgments

Supported by: NIH Grants R21AI112722 (B.KE) and R01DK102110 (J.W.KW), National Natural Science Foundation of China 81270558 (Q.XIA) and 81470895 (M.Zhang), and The Dumont Research Foundation.

## Abbreviations

| | |
|---|---|
| **β-catenin$^{FL/FL}$** | floxed β-catenin |
| **β-catenin$^{M-KO}$** | myeloid-specific β-catenin knockout |
| **CRISPR** | clustered regularly interspaced short palindromic repeats |
| **Cas9** | CRISPR associated protein 9 |
| **HSF1** | heat shock transcription factor 1 |
| **HSF1$^{FL/FL}$** | floxed HSF1 |
| **HSF1$^{M-KO}$** | myeloid-specific HSF1 knockout |
| **IRI** | ischemia/reperfusion injury |
| **ROS** | reactive oxygen species |
| **sALT** | serum alanine aminotransferase |
| **siRNA** | small interfering RNA |
| **XBP1** | X-box-binding protein |

## References

1. Zhai Y, Busuttil RW, Kupiec-Weglinski JW. Liver ischemia and reperfusion injury: new insights into mechanisms of innate-adaptive immune-mediated tissue inflammation. Am J Transplant. 2011; 11:1563–1569. [PubMed: 21668640]
2. Jaeschke H, Woolbright BL. Current strategies to minimize hepatic ischemia-reperfusion injury by targeting reactive oxygen species. Transplant Rev (Orlando). 2012; 26:103–114. [PubMed: 22459037]
3. Tschopp J, Schroder K. NLRP3 inflammasome activation: The convergence of multiple signalling pathways on ROS production? Nat Rev Immunol. 2010; 10:210–215. [PubMed: 20168318]
4. Eltzschig HK, Eckle T. Ischemia and reperfusion--from mechanism to translation. Nat Med. 2011; 17:1391–1401. [PubMed: 22064429]
5. Martinon F, Mayor A, Tschopp J. The inflammasomes: guardians of the body. Annu Rev Immunol. 2009; 27:229–265. [PubMed: 19302040]
6. Dostert C, Petrilli V, Van Bruggen R, Steele C, Mossman BT, Tschopp J. Innate immune activation through Nalp3 inflammasome sensing of asbestos and silica. Science. 2008; 320:674–677. [PubMed: 18403674]
7. Mariathasan S, Newton K, Monack DM, Vucic D, French DM, Lee WP, Roose-Girma M, et al. Differential activation of the inflammasome by caspase-1 adaptors ASC and Ipaf. Nature. 2004; 430:213–218. [PubMed: 15190255]
8. Kastner DL, Aksentijevich I, Goldbach-Mansky R. Autoinflammatory disease reloaded: a clinical perspective. Cell. 2010; 140:784–790. [PubMed: 20303869]
9. Mariathasan S, Monack DM. Inflammasome adaptors and sensors: intracellular regulators of infection and inflammation. Nat Rev Immunol. 2007; 7:31–40. [PubMed: 17186029]

10. Huang H, Chen HW, Evankovich J, Yan W, Rosborough BR, Nace GW, Ding Q, et al. Histones activate the NLRP3 inflammasome in Kupffer cells during sterile inflammatory liver injury. J Immunol. 2013; 191:2665–2679. [PubMed: 23904166]
11. Akerfelt M, Morimoto RI, Sistonen L. Heat shock factors: integrators of cell stress, development and lifespan. Nat Rev Mol Cell Biol. 2010; 11:545–555. [PubMed: 20628411]
12. Anckar J, Sistonen L. Heat shock factor 1 as a coordinator of stress and developmental pathways. Adv Exp Med Biol. 2007; 594:78–88. [PubMed: 17205677]
13. Zhang L, Jiang H, Gao X, Zou Y, Liu M, Liang Y, Yu Y, et al. Heat shock transcription factor-1 inhibits H2O2-induced apoptosis via down-regulation of reactive oxygen species in cardiac myocytes. Mol Cell Biochem. 2011; 347:21–28. [PubMed: 20941531]
14. Zhang H, Zhang L, Yu F, Liu Y, Liang Q, Deng G, Chen G, et al. HSF1 is a transcriptional activator of IL-10 gene expression in RAW264.7 macrophages. Inflammation. 2012; 35:1558–1566. [PubMed: 22549481]
15. Tanaka K, Namba T, Arai Y, Fujimoto M, Adachi H, Sobue G, Takeuchi K, et al. Genetic evidence for a protective role for heat shock factor 1 and heat shock protein 70 against colitis. J Biol Chem. 2007; 282:23240–23252. [PubMed: 17556362]
16. Murapa P, Ward MR, Gandhapudi SK, Woodward JG, D'Orazio SE. Heat shock factor 1 protects mice from rapid death during Listeria monocytogenes infection by regulating expression of tumor necrosis factor alpha during fever. Infect Immun. 2011; 79:177–184. [PubMed: 20956571]
17. Ambade A, Catalano D, Lim A, Mandrekar P. Inhibition of heat shock protein (molecular weight 90 kDa) attenuates proinflammatory cytokines and prevents lipopolysaccharide-induced liver injury in mice. Hepatology. 2012; 55:1585–1595. [PubMed: 22105779]
18. Ke B, Shen XD, Kamo N, Ji H, Yue S, Gao F, Busuttil RW, et al. beta-catenin regulates innate and adaptive immunity in mouse liver ischemia-reperfusion injury. Hepatology. 2013; 57:1203–1214. [PubMed: 23081841]
19. Martinon F, Chen X, Lee AH, Glimcher LH. TLR activation of the transcription factor XBP1 regulates innate immune responses in macrophages. Nat Immunol. 2010; 11:411–418. [PubMed: 20351694]
20. West AP, Brodsky IE, Rahner C, Woo DK, Erdjument-Bromage H, Tempst P, Walsh MC, et al. TLR signalling augments macrophage bactericidal activity through mitochondrial ROS. Nature. 2011; 472:476–480. [PubMed: 21525932]
21. Kamo N, Ke B, Ghaffari AA, Shen XD, Busuttil RW, Cheng G, Kupiec-Weglinski JW. ASC/caspase-1/IL-1beta signaling triggers inflammatory responses by promoting HMGB1 induction in liver ischemia/reperfusion injury. Hepatology. 2013; 58:351–362. [PubMed: 23408710]
22. Neef DW, Jaeger AM, Thiele DJ. Heat shock transcription factor 1 as a therapeutic target in neurodegenerative diseases. Nat Rev Drug Discov. 2011; 10:930–944. [PubMed: 22129991]
23. Shen XD, Ke B, Zhai Y, Amersi F, Gao F, Anselmo DM, Busuttil RW, et al. CD154-CD40 T-cell costimulation pathway is required in the mechanism of hepatic ischemia/reperfusion injury, and its blockade facilitates and depends on heme oxygenase-1 mediated cytoprotection. Transplantation. 2002; 74:315–319. [PubMed: 12177608]
24. Rao J, Yue S, Fu Y, Zhu J, Wang X, Busuttil RW, Kupiec-Weglinski JW, et al. ATF6 mediates a pro-inflammatory synergy between ER stress and TLR activation in the pathogenesis of liver ischemia-reperfusion injury. Am J Transplant. 2014; 14:1552–1561. [PubMed: 24903305]
25. Suzuki S, Toledo-Pereyra LH, Rodriguez FJ, Cejalvo D. Neutrophil infiltration as an important factor in liver ischemia and reperfusion injury. Modulating effects of FK506 and cyclosporine. Transplantation. 1993; 55:1265–1272. [PubMed: 7685932]
26. Ke B, Shen XD, Zhang Y, Ji H, Gao F, Yue S, Kamo N, et al. KEAP1-NRF2 complex in ischemia-induced hepatocellular damage of mouse liver transplants. J Hepatol. 2013; 59:1200–1207. [PubMed: 23867319]
27. Kim H, Wu J, Ye S, Tai CI, Zhou X, Yan H, Li P, et al. Modulation of beta-catenin function maintains mouse epiblast stem cell and human embryonic stem cell self-renewal. Nat Commun. 2013; 4:2403. [PubMed: 23985566]
28. Sanjana NE, Shalem O, Zhang F. Improved vectors and genome-wide libraries for CRISPR screening. Nat Methods. 2014; 11:783–784. [PubMed: 25075903]

29. Froh M, Konno A, Thurman RG. Isolation of liver Kupffer cells. Curr Protoc Toxicol. 2003; Chapter 14(Unit14):14.
30. Ke B, Shen XD, Gao F, Ji H, Qiao B, Zhai Y, Farmer DG, et al. Adoptive transfer of ex vivo HO-1 modified bone marrow-derived macrophages prevents liver ischemia and reperfusion injury. Mol Ther. 2010; 18:1019–1025. [PubMed: 20029397]
31. Yu SS, Lau CM, Barham WJ, Onishko HM, Nelson CE, Li H, Smith CA, et al. Macrophage-specific RNA interference targeting via “click”, mannosylated polymeric micelles. Mol Pharm. 2013; 10:975–987. [PubMed: 23331322]
32. Fang D, Hawke D, Zheng Y, Xia Y, Meisenhelder J, Nika H, Mills GB, et al. Phosphorylation of beta-catenin by AKT promotes beta-catenin transcriptional activity. J Biol Chem. 2007; 282:11221–11229. [PubMed: 17287208]
33. Zhou R, Yazdi AS, Menu P, Tschopp J. A role for mitochondria in NLRP3 inflammasome activation. Nature. 2011; 469:221–225. [PubMed: 21124315]
34. Schroder K, Tschopp J. The inflammasomes. Cell. 2010; 140:821–832. [PubMed: 20303873]
35. Akira S, Uematsu S, Takeuchi O. Pathogen recognition and innate immunity. Cell. 2006; 124:783–801. [PubMed: 16497588]
36. Rathinam VA, Vanaja SK, Waggoner L, Sokolovska A, Becker C, Stuart LM, Leong JM, et al. TRIF licenses caspase-11-dependent NLRP3 inflammasome activation by gram-negative bacteria. Cell. 2012; 150:606–619. [PubMed: 22819539]
37. Qiu Q, Zheng Z, Chang L, Zhao YS, Tan C, Dandekar A, Zhang Z, et al. Toll-like receptor-mediated IRE1alpha activation as a therapeutic target for inflammatory arthritis. EMBO J. 2013; 32:2477–2490. [PubMed: 23942232]
38. Eltzschig HK, Bratton DL, Colgan SP. Targeting hypoxia signalling for the treatment of ischaemic and inflammatory diseases. Nat Rev Drug Discov. 2014; 13:852–869. [PubMed: 25359381]
39. Peyssonnaux C, Cejudo-Martin P, Doedens A, Zinkernagel AS, Johnson RS, Nizet V. Cutting edge: Essential role of hypoxia inducible factor-1alpha in development of lipopolysaccharide-induced sepsis. J Immunol. 2007; 178:7516–7519. [PubMed: 17548584]
40. Idzko M, Ferrari D, Eltzschig HK. Nucleotide signalling during inflammation. Nature. 2014; 509:310–317. [PubMed: 24828189]
41. Mariathasan S, Weiss DS, Newton K, McBride J, O’Rourke K, Roose-Girma M, Lee WP, et al. Cryopyrin activates the inflammasome in response to toxins and ATP. Nature. 2006; 440:228–232. [PubMed: 16407890]
42. Calfon M, Zeng H, Urano F, Till JH, Hubbard SR, Harding HP, Clark SG, et al. IRE1 couples endoplasmic reticulum load to secretory capacity by processing the XBP-1 mRNA. Nature. 2002; 415:92–96. [PubMed: 11780124]
43. Yoshida H, Matsui T, Yamamoto A, Okada T, Mori K. XBP1 mRNA is induced by ATF6 and spliced by IRE1 in response to ER stress to produce a highly active transcription factor. Cell. 2001; 107:881–891. [PubMed: 11779464]
44. Yamamoto M, Sato S, Hemmi H, Hoshino K, Kaisho T, Sanjo H, Takeuchi O, et al. Role of adaptor TRIF in the MyD88-independent toll-like receptor signaling pathway. Science. 2003; 301:640–643. [PubMed: 12855817]
45. Li Q, Harraz MM, Zhou W, Zhang LN, Ding W, Zhang Y, Eggleston T, et al. Nox2 and Rac1 regulate H2O2-dependent recruitment of TRAF6 to endosomal interleukin-1 receptor complexes. Mol Cell Biol. 2006; 26:140–154. [PubMed: 16354686]
46. Lerner AG, Upton JP, Praveen PV, Ghosh R, Nakagawa Y, Igbaria A, Shen S, et al. IRE1alpha induces thioredoxin-interacting protein to activate the NLRP3 inflammasome and promote programmed cell death under irremediable ER stress. Cell Metab. 2012; 16:250–264. [PubMed: 22883233]
47. Overley-Adamson B, Artlett CM, Stephens C, Sassi-Gaha S, Weis RD, Thacker JD. Targeting the unfolded protein response, XBP1, and the NLRP3 inflammasome in fibrosis and cancer. Cancer Biol Ther. 2014; 15:452–462. [PubMed: 24496016]
48. Neef DW, Turski ML, Thiele DJ. Modulation of heat shock transcription factor 1 as a therapeutic target for small molecule intervention in neurodegenerative disease. PLoS Biol. 2010; 8:e1000291. [PubMed: 20098725]

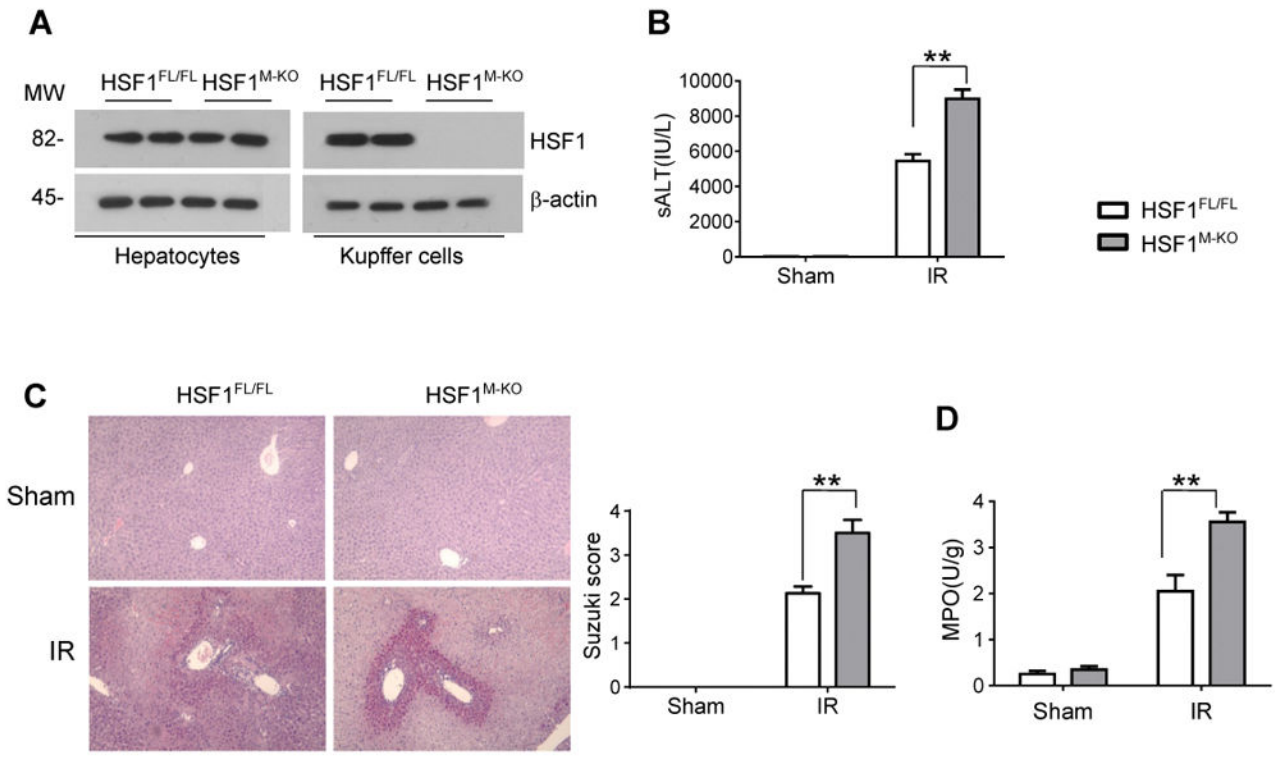


**Figure 1. Myeloid-specific HSF1 deficiency increases hepatocellular damage in liver IRI**

Mice were subjected to 90min of partial liver warm ischemia, followed by 6h of reperfusion. (A) Western blots for detection of HSF1 in hepatocytes and liver Kupffer cells. Representative of three experiments. (B) Hepatocellular function in serum samples was evaluated by sALT levels (IU/L). Results expressed as mean±SD (n=4–6 samples/group). **p<0.01. (C) Representative histological staining (H&E) of ischemic liver tissue. Results representative of 4–6 mice/group; original magnification ×100. Liver damage, evaluated by Suzuki's histological score. **p<0.01. (D) Liver neutrophil accumulation, analyzed by MPO activity (U/g). Mean±SD (n=4–6 samples/group). **p<0.01.

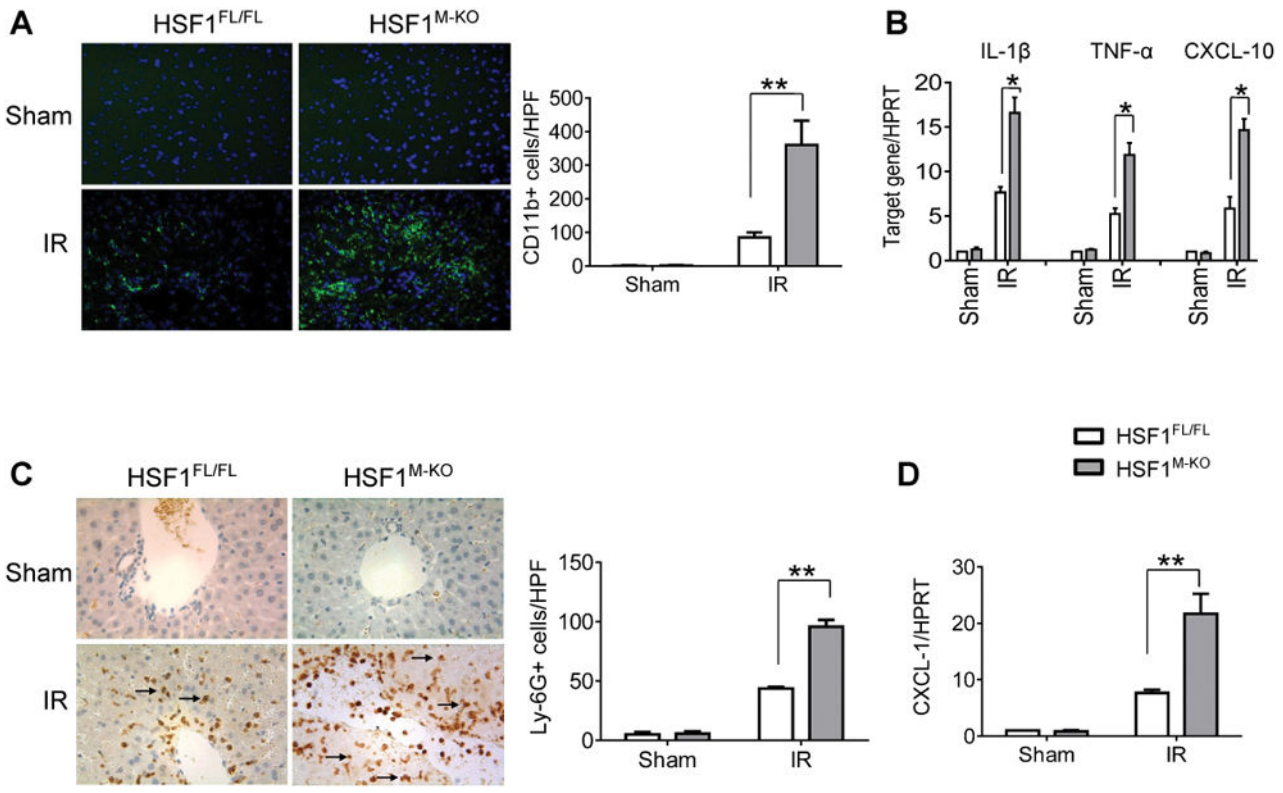


**Figure 2. Myeloid-specific HSF1 deficiency increases macrophage/neutrophil trafficking and proinflammatory mediators in IR-stressed liver**

Liver macrophages and neutrophils were detected by immunohistochemical staining using mAbs against mouse $CD11b^+$ and Ly6G in $HSF1^{FL/FL}$ ( □) and $HSF1^{M\text{-}KO}$ ( ■) mice. (A) Immunohistochemical staining of $CD11b^+$ macrophages in ischemic livers. Quantification of $CD11b^+$ macrophages per high power field. Results scored semi-quantitatively by averaging number of positively-stained cells (mean±SD)/field at 200×magnification. Representative of 4–6 mice/group. **p<0.01. (B) Quantitative RT-PCR-assisted detection of IL-1β, TNF-α, and CXCL-10 in mouse livers. Each column represents the mean±SD (n=3–4 samples/group). *p<0.05. (C) Immunohistochemical staining of $Ly6G^+$ neutrophils in ischemic livers. Quantification of $Ly6G^+$ neutrophils per high power field (original magnification ×200). Representative of 4–6 mice/group. **p<0.01. (D) Quantitative RT-PCR-assisted detection of CXCL-1 in mouse livers. Each column represents the mean±SD (n=3–4 samples/group). **p<0.01.

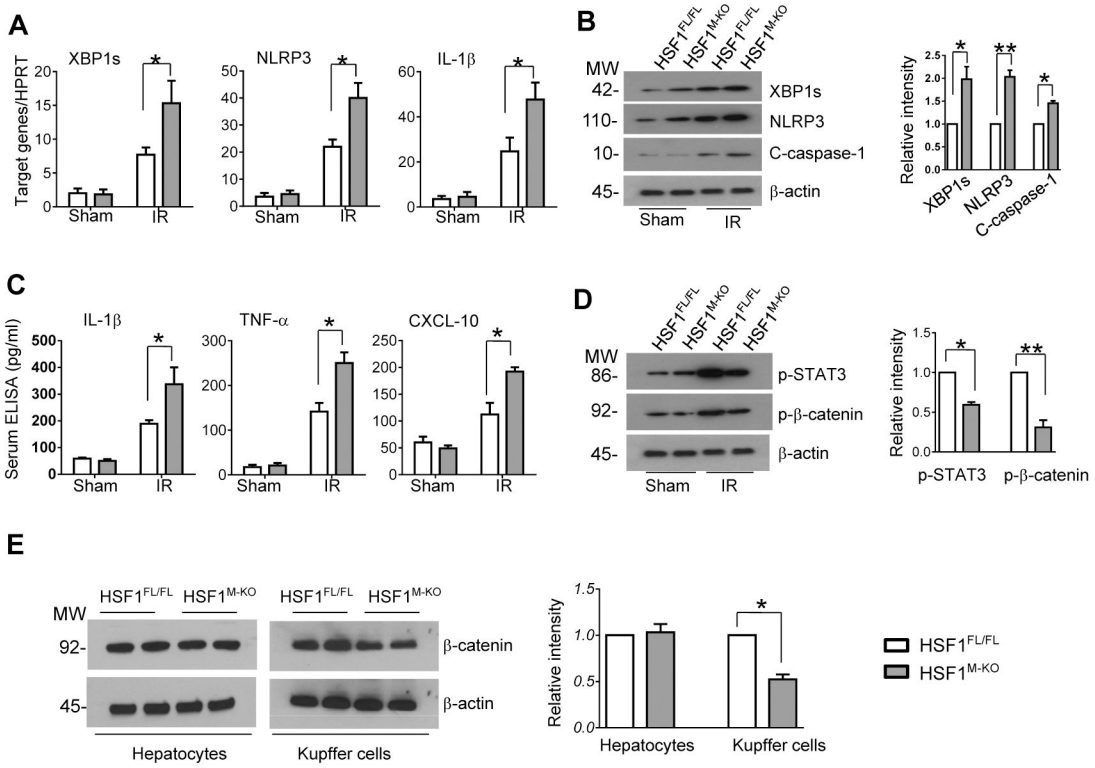


**Figure 3. Myeloid-specific HSF1 deficiency depresses β-catenin signaling and enhances XBP1/NLRP3 activation in IR-stressed liver**

(A) Quantitative RT-PCR-assisted detection of mRNA coding for XBP1s, NLRP3, and IL-1β in mouse livers. Each column represents the mean±SD (n=3–4 samples/group). *p<0.05. (B) Western-assisted analysis and relative density ratio of XBP1s, NLRP3 and cleaved caspase-1. Representative of three experiments. *p<0.05, **p<0.01. (C) ELISA analysis of IL-β, TNF-α, and CXCL-10 levels in animal serum. Mean±SD (n=3–4 samples/group), *p<0.05. (D) Western blot analysis and relative density ratio of p-Stat3 and β-catenin. Representative of three experiments. *p<0.05, **p<0.01. (E) Western-assisted analysis and relative density ratio of β-catenin in hepatocytes and liver Kupffer cells. Representative of three experiments. *p<0.05, **p<0.01.

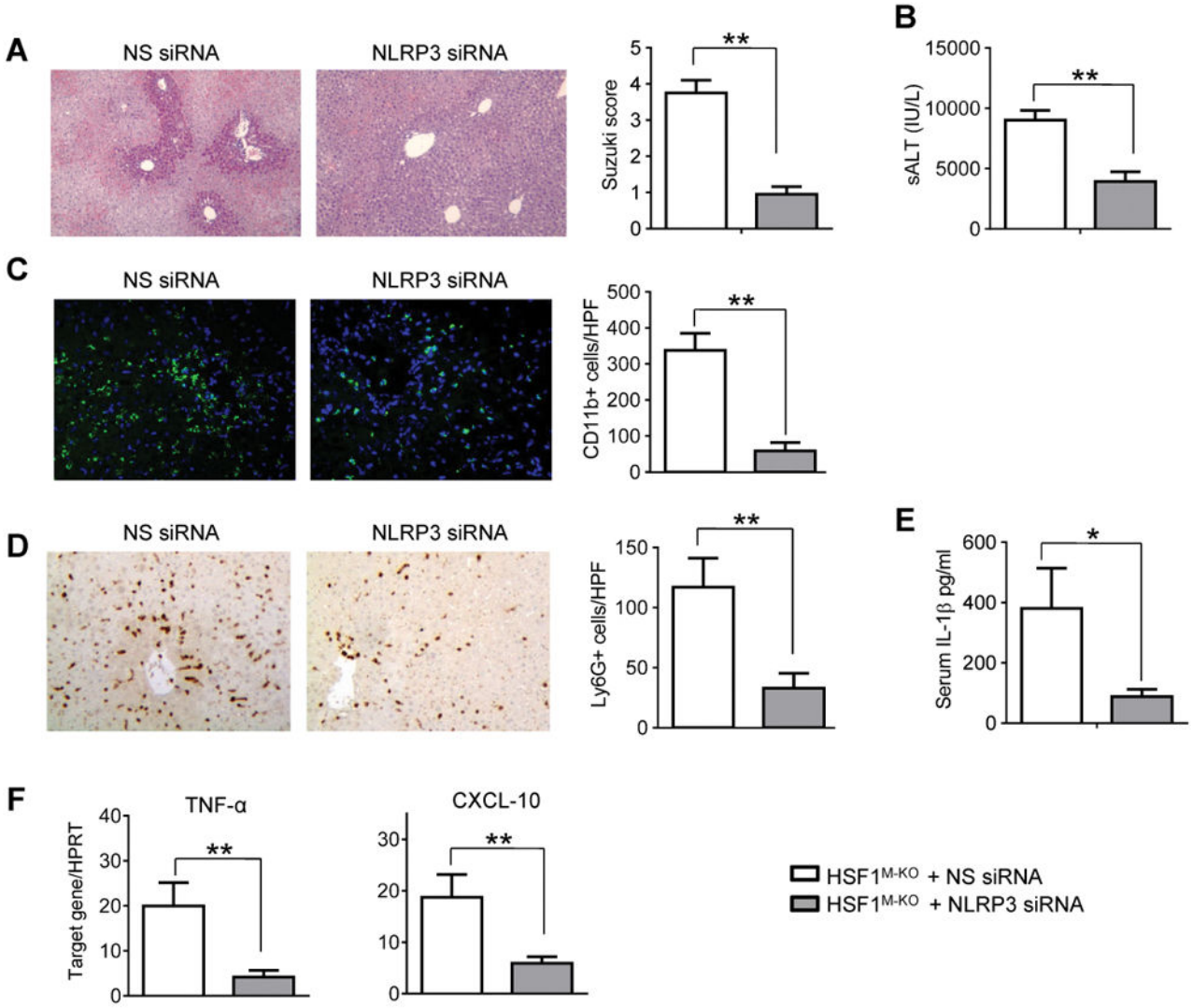


**Figure 4. NLRP3 activation in myeloid HSF1-deficient liver contributes to IR-triggered liver inflammation**

The HSF1$^{M\text{-}KO}$ mice were injected via tail vein with AlexaFluor488-labeled nonspecific (NS) control siRNAs ( ▭ ) or NLRP3 siRNA ( ▬ ) (2 mg/kg) mixed with mannose-conjugated polymers at 4 h prior to ischemia. (A) Representative histological staining (H&E) of ischemic liver tissue. Results representative of 4–6 mice/group; original magnification ×100. The severity of liver IRI was evaluated by the Suzuki's histological grading. **p<0.01. (B) Hepatocellular function was evaluated by sALT levels (IU/L). Results expressed as mean±SD (n=4–6 samples/group). **p<0.01. (C) Immunohistochemical staining of CD11b$^+$ macrophages in ischemic livers. Quantification of CD11b$^+$ macrophages per high power field. Results scored semi-quantitatively by averaging number of positively-stained cells (mean±SD)/field at 200×magnification. Representative of 4–6 mice/group. **p<0.01. (D) Immunohistochemical staining of Ly6G$^+$ neutrophils in ischemic livers. Quantification of Ly6G$^+$ neutrophils per high power field (original magnification ×200). Representative of 4–6 mice/group. **p<0.01. (E) ELISA analysis of

IL-β levels in animal serum. Mean±SD (n=3–4 samples/group), *p<0.05. (F) Quantitative RT-PCR-assisted detection of mRNA coding for TNF-α and CXCL-10. Each column represents the mean±SD (n=3–4 samples/group). **p<0.01.

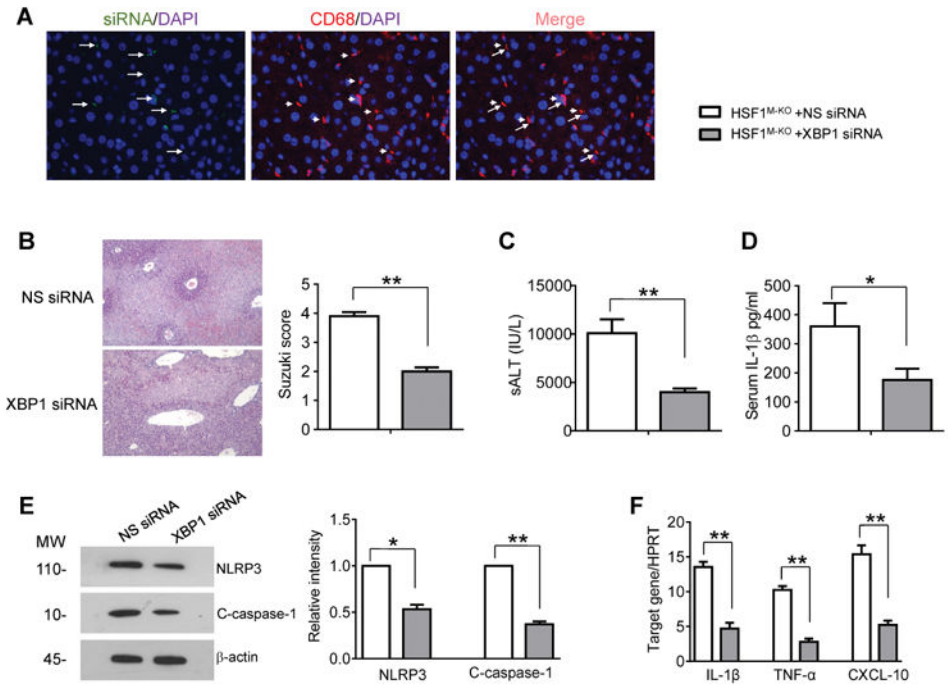


**Figure 5. XBP1 is required for NLRP3 activation in myeloid HSF1-deficient liver in response to IR**

The HSF1$^{M\text{-}KO}$ mice were injected via tail vein with AlexaFluor488-labeled nonspecific (NS) control siRNAs ( ▭ ) or XBP1 siRNA ( ▬ ) (2 mg/kg) mixed with mannose-conjugated polymers at 4 h prior to ischemia. (A) Immunofluorescence staining of AlexaFluor488-labeled control siRNA (long arrow) and CD68 positive macrophages (short arrow) in ischemic liver lobes. Note: Green: AlexaFluor488-labeled siRNA; red: macrophage marker detected with CD68 mAb; blue: DAPI nuclear stain. Original magnification ×200; Representative of 3–4 mice/group (B) Representative histological staining (H&E) of ischemic liver tissue. Results representative of 4–6 mice/group; original magnification ×100. The severity of liver IRI was evaluated by the Suzuki's histological grading. **p<0.01. (C) Hepatocellular function was evaluated by sALT levels (IU/L). Results expressed as mean ±SD (n=4–6 samples/group). **p<0.01. (D) ELISA analysis of IL-β levels in animal serum. Mean±SD (n=3–4 samples/group), *p<0.05. (E) Western blots analysis and relative density ratio of NLRP3 and cleaved caspase-1. Representative of three experiments. *p<0.05, **p<0.01. (F) Quantitative RT-PCR-assisted detection of mRNA coding for IL-1β, TNF-α, and CXCL-10. Each column represents the mean±SD (n=3–4 samples/group). **p<0.01.

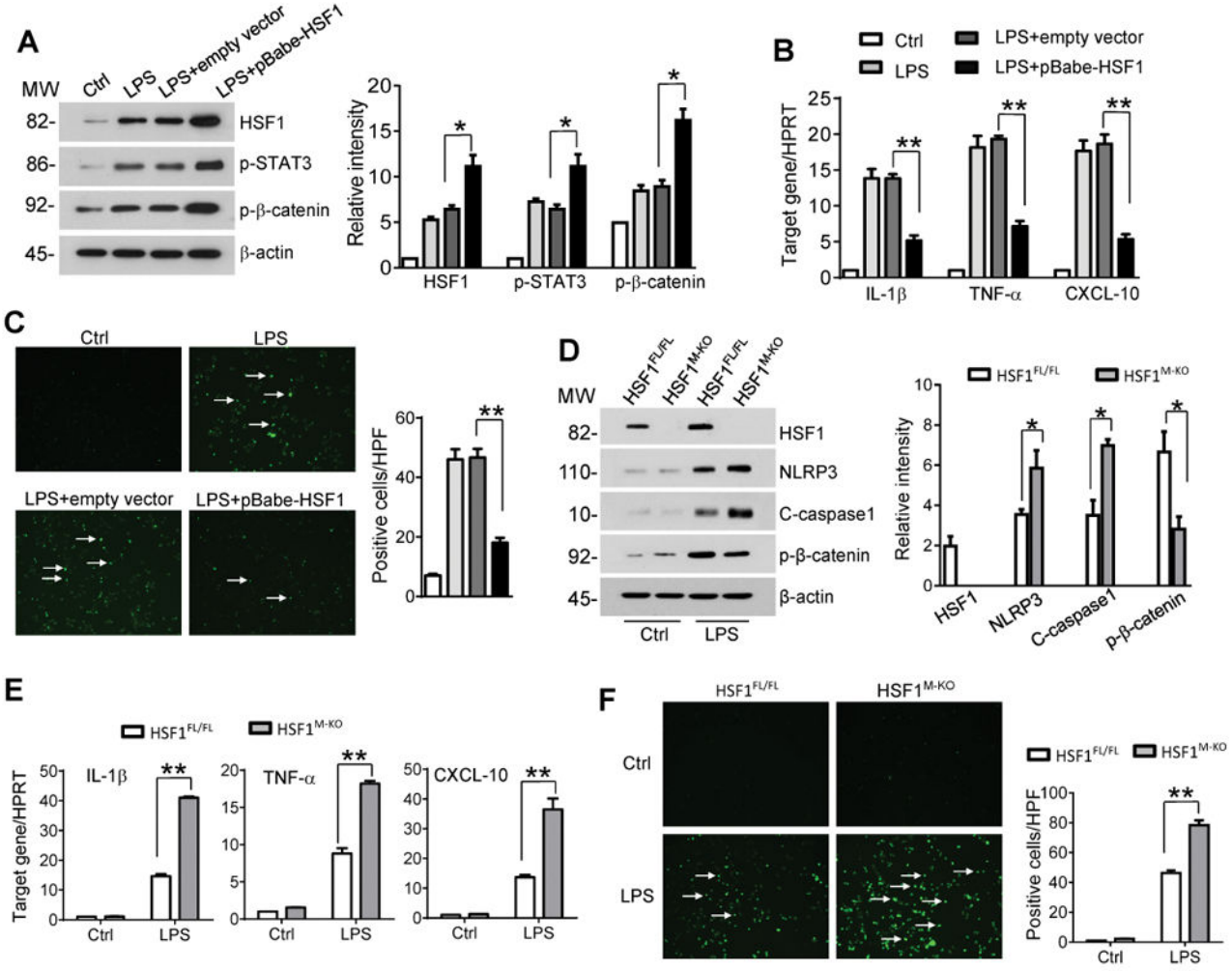


**Figure 6. Disruption of myeloid HSF1 inhibits β-catenin activity but enhances NLRP3 inflammasome activation in macrophages**

(A) Murine bone marrow-derived macrophages (BMMs) from wild type (WT) mice were transfected with control vector ( ▭ ) or pBabe-HSF1 ( ▬ ) followed by LPS (100ng/ml) stimulation. (A) Western blot analysis and relative density ratio of HSF1, p-Stat3 and p-β-catenin. Representative of three experiments. *p<0.05. (B) Quantitative RT-PCR-assisted detection of mRNA coding for IL-1β, TNF-α, and CXCL-10. Each column represents mean ±SD (n=3–4 samples/group). **p<0.01. (C) ROS production was detected by Carboxy-H2DFFDA in LPS-stimulated BMMs from WT mice. Positive green fluorescent-labeled cells were counted blindly in 10 HPF/section (×200). Quantification of ROS-producing BMMs (green) per high power field (×200). **p<0.01. (D) BMMs from $HSF1^{FL/FL}$ ( ▭ ) and $HSF1^{M\text{-}KO}$ ( ▬ ) mice were incubated with LPS (100 ng/ml). Western-assisted analysis and relative density ratio of HSF1, NLRP3, cleaved caspase-1, and p-β-catenin in LPS-stimulated cells. Representative of three experiments. *p<0.05. (E) Quantitative RT-PCR-assisted detection of mRNA coding for IL-1β, TNF-α, and CXCL-10. Each column represents mean±SD (n=3–4 samples/group). **p<0.01. (F) ROS production was detected by Carboxy-H2DFFDA in LPS-stimulated BMMs from $HSF1^{FL/FL}$ and $HSF1^{M\text{-}KO}$ mice.

Positive green fluorescent-labeled cells were counted blindly in 10 HPF/section (×200). Quantification of ROS-producing BMMs (green) per high power field (×200). **p<0.01.

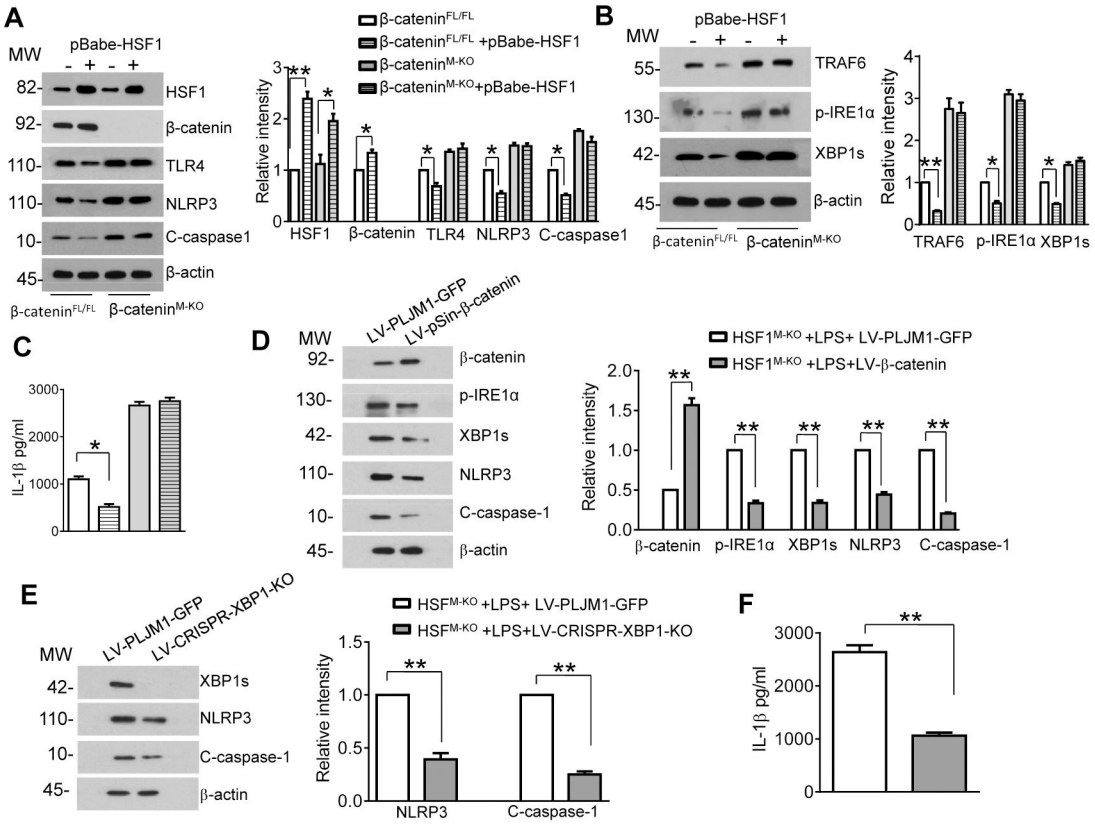


**Figure 7. Myeloid β-catenin signaling is essential for the HSF1-mediated immune regulation of XBP1-dependent NLRP3 activation in macrophages**

BMMs from β-catenin$^{FL/FL}$ ( ▭ ) and β-catenin$^{M-KO}$ ( ▬ ) mice were transfected with pBabe-HSF1 or control vector followed by LPS (100 ng/ml) stimulation. (A) Western-assisted analysis and relative density ratio of HSF1, β-catenin, and TLR4, NLRP3, and cleaved caspase-1. Representative of three experiments. *p<0.05, **p<0.01. (B) Western blot analysis and their relative density ratio of TRAF6, p-IRE1α, and XBP1s. Representative of three experiments. *p<0.05, **p<0.01. (C) ELISA-assisted production of IL-1β in cell culture supernatants. Mean±SD (n=3–4 samples/group). *p< 0.05. (D) BMMs from HSF1$^{M-KO}$ mice were transduced with lentivirus-expressing β-catenin (LV-pSin-β-catenin ( ▬ ), LV-CRISPR/Cas9 XBP1 knockout (KO) ( ■ ), or LV-pLJM1-GFP controls ( ▭ ). After 24–48 h, cells were supplemented with 100 ng/ml of LPS for additional 6 h. Western blot analysis and their relative density ratio of β-catenin, p-IRE1α, XBP1s, NLRP3, and cleaved caspase-1 in LV-pSin-β-catenin- or LV-pLJM1-GFP-transduced cells. Representative of three experiments. **p<0.01. (E) Western blot analysis and their relative density ratio of XBP1s, NLRP3, and cleaved caspase-1 in LV-CRISPR/Cas9-XBP1 KO- or LV-pLJM1-GFP-transduced cells. Representative of three experiments. **p<0.01. (F) ELISA-assisted production of IL-β in cell culture supernatants. Mean±SD (n=3–4 samples/group). **p< 0.01.

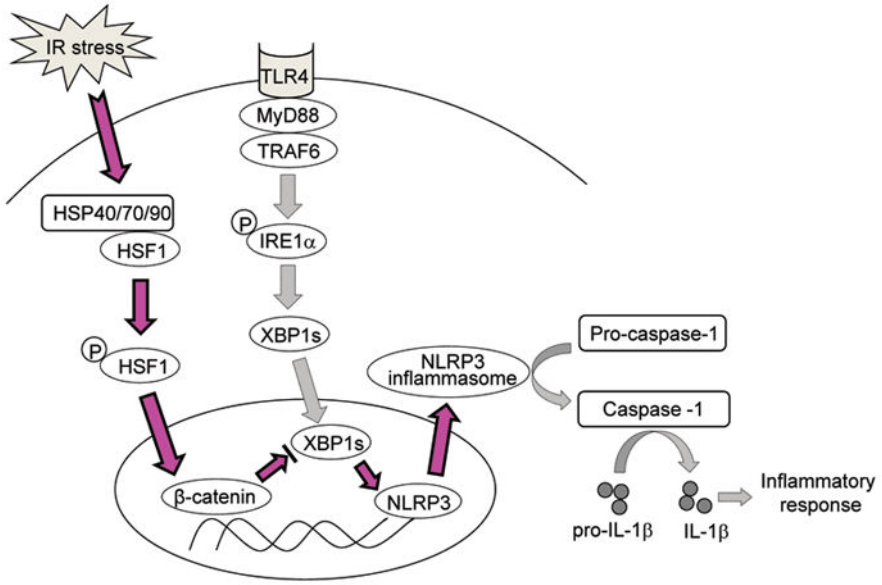


**Figure 8. Schematic illustration of HSF1-β-catenin axis in the regulation of innate immune response in IR-stressed liver inflammation**

This novel signaling pathway is indicated by the solid pink arrow. HSF1 can be induced in IR-stressed livers. HSF1 induction increases β-catenin translocation from the cytoplasm to the nucleus, resulting in enhanced β-catenin transcriptional activity, which inhibits XBP1 activation in response to TLR/TRAF6 stimulation in macrophages. Moreover, suppression of XBP1 activity diminishes NLRP3 functions, leading to reduced caspase-1 activation, and the maturation and secretion of IL-1β in liver IRI.